A numerical procedure for the pushover analysis of masonry towers

Massimiliano Bocciarelli*, Gaia Barbieri

Architecture, Built Environment and Construction Engineering Department, Politecnico di Milano (Technical University), piazza Leonardo da Vinci 32, 20133, Italy

In this paper, a numerical approach for the pushover analysis of masonry towers, having hollow arbitrary sections, is proposed. Masonry is considered a nonlinear softening material in compression and brittle in tension. The tower, modeled in the framework of the Euler-Bernoulli beam theory, is subjected to a predefined load distribution, but the problem is formulated as a displacement controlled analysis in order to follow the post peak descending branch of the structural response. Nonlinear geometric effects and nonlinear constraints (the latter due to surrounding buildings) are also considered. Benchmarking pushover analyses are performed with the commercial code Abaqus in relation to a real case (the Gabbia Tower in Mantua), which proved the accuracy and reliability of the results obtained with the present formulation and the noteworthy reduction of computing time.

Keywords:
Masonry tower
Pushover analysis
Plastic hinge length
Computing time
Probabilistic analysis

1. Introduction

Many historical buildings are constituted by unreinforced masonry and are characterized by a high seismic vulnerability. Indeed, these structures were conceived to withstand the effects of gravity loads but were not provided for adequate lateral resistance and ductility against horizontal loads, such as those induced by an earthquake [1–4].

The analysis of masonry structures is very complex in view of their heterogeneity and uncertainty typical of the constituent materials. Masonry is a non-homogeneous, non-isotropic material, with a mechanical behavior dominated by the nonlinear phase, characterized by negligible strength and brittleness in tension, and dissipative with softening behavior in compression [5].

For these features, the seismic vulnerability of masonry buildings is rarely assessed by linear elastic analysis procedures. Nonlinear dynamic analysis methods represent in principle the most reliable tool. Nevertheless, they are very complex and require a great amount of computational resources and time [6,7] and further research efforts are still needed, before they can be confidently used in standard design [8]. Therefore, nonlinear static (pushover) procedures have been increasingly recognized as effective tools in seismic design and vulnerability assessment: they provide information on both the strength and ductility of the structure, while preserving the simplicity of a static analysis [9,10]. The main outcome consists in the curve relating the displacement of a certain point (named controlling point) to the resultant of a predefined horizontal distributed force applied to the structure. This curve, representing the seismic capacity of the structure, is then compared with the seismic demand, expressed in terms of response spectrum, through specific procedures as the N2 or the capacity spectrum method [11,12].

Due to their increasingly relevant role, several seismic codes and recommendations have recently extended the application of pushover-based methods to existing and monumental masonry buildings [13,14].

Currently, several studies are available in literature dealing with the seismic vulnerability assessment of historical masonry buildings by means of pushover analyses, e.g. [15–19], and in particular of ancient towers [20–22]. It is well recognized that these pushover-based methods may be affected by inaccuracy when applied to structures whose failure mechanisms are influ-enced by the higher modes of vibration [7,23,24]. For this reason, improved multi-modal pushover analyses were developed, which combine the results obtained using the inertia force distribution related to different modes, see e.g. [25].

A key point, when dealing with pushover analysis of masonry structures, is the determination of the ultimate displacement in the capacity curve. In [13] it is suggested that this is achieved when, in the descending branch, the 85% of the maximum force is reached. This criterion requires the implementation of a softening branch in the masonry constitutive law (perfect plastic models would lead to unrealistic high ductility), and consequently the need to perform force drive pushover analyses with displacement control.

This paper presents a simple and efficient numerical approach for the pushover analysis of masonry towers, having hollow

* Corresponding author.
E-mail address: massimiliano.bocciarelli@polimi.it (M. Bocciarelli).

©2017. This manuscript version is made available under the CC-BY-NC-ND 4.0 license http://creativecommons.org/licenses/by-nc-nd/4.0/
Published Journal Article available at: http://dx.doi.org/10.1016/j.soildyn.2016.07.022

arbitrary sections. It is assumed that masonry behaves as non-linear material with dissipative and softening behavior and the structure is modeled in the framework of the Euler-Bernoulli beam theory. A specific topological algorithm is formulated in order to derive, from the three dimensional model of the tower, a bi-dimensional discretization of each section, which is then adopted to construct its moment-curvature curve. Nonlinear geometric effects and the presence of constraints, due to surrounding buildings and governed by nonlinear relationships in terms of displacement versus reaction force, are also considered. The load distribution is assigned as inverted triangular (however, the formulation can deal with any type of load distribution), and the problem is formulated in terms of monotonically increasing quantities, as primary unknowns, such as the section curvatures, in order to follow the post peak softening branch of the structural response. In classical FEM codes this type of analysis can be performed by means of arc-length type procedures, see [26]. To avoid curvature localization, induced by the masonry softening behavior, the concept of plastic hinge is introduced and the determination of its length is dealt with by comparison with classical 3D nonlinear finite element analyses.

Soil is not directly considered in the present model. However, its effect enters in the definition of the seismic demand, through proper coefficients depending on the soil constitution and defined according to seismic codes. The pounding effect, which could be one of the main causes of severe building damages during earthquake, is not considered in the present formulation.

A case study is then proposed, the Gabbia Tower in Mantua, and benchmarking pushover analyses are performed with the commercial code Abaqus [27], whose results are used to validate the numerical procedure. This example also allowed to point out the great reduction of computing time achieved with the proposed approach.

2. Numerical procedure

2.1. Constitutive equations

Masonry in compression is modeled by an elasto-plastic stress-strain relationship with limited ductility and softening, already adopted in other studies, see [6,8,28]. The behavior under tensile stresses is assumed to be linear elastic up to the tensile strength, followed by a linear softening branch down to zero, see Eq. (1) and Fig. 1.

$$\sigma_m = \begin{cases} 0 & \text{if } \varepsilon_m \geq \varepsilon_{mtu} \\ f_{mt}\cdot(\varepsilon_{mtu} - \varepsilon_m)/(\varepsilon_{mtu} - \varepsilon_{mt1}) & \text{if } \varepsilon_{mt1} \leq \varepsilon_m < \varepsilon_{mtu} \\ E_m\varepsilon_m & \text{if } -\varepsilon_{mc1} \leq \varepsilon_m < \varepsilon_{mt1} \\ -f_{mc} & \text{if } -\varepsilon_{mc2} \leq \varepsilon_m < -\varepsilon_{mc1} \\ -f_{mc}\cdot(\varepsilon_{mcu} + \varepsilon_m)/(\varepsilon_{mcu} - \varepsilon_{mc2}) & \text{if } -\varepsilon_{mcu} \leq \varepsilon_m < -\varepsilon_{mc2} \\ 0 & \text{if } \varepsilon_m < -\varepsilon_{mcu} \end{cases} \quad (1)$$

where: E_m is the Young modulus, $\varepsilon_{mc1} = f_{mc}/E_m$ is the strain corresponding to the compressive strength f_{mc}, $\varepsilon_{mc2} = \mu_1\varepsilon_{mc1}$ is the strain at the end of the plateau, $\varepsilon_{mcu} = \mu_2\varepsilon_{mc2}$ is the ultimate compressive strain at the end of the softening branch, $\varepsilon_{mt1} = f_{mt}/E_m$ and ε_{mtu} represent the strain at the tensile peak stress f_{mt} and the ultimate tensile strain, respectively. In Eq. (1) the sign $-$ is introduced since all material properties are assumed to be positive, while stress σ_m and strain ε_m are positive if tensile and negative if compressive.

Masonry towers are frequently surrounded by other buildings, whose effect is here modeled, in a simplified manner consistent with the assumption of Euler-Bernoulli beam theory, as a series of

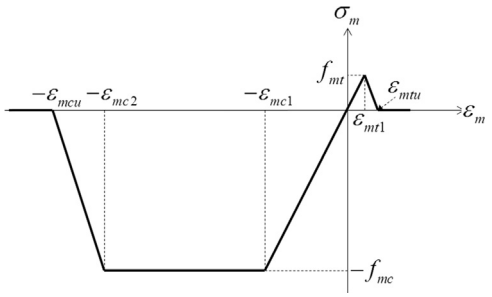

Fig. 1. Stress-strain relationship assumed for masonry.

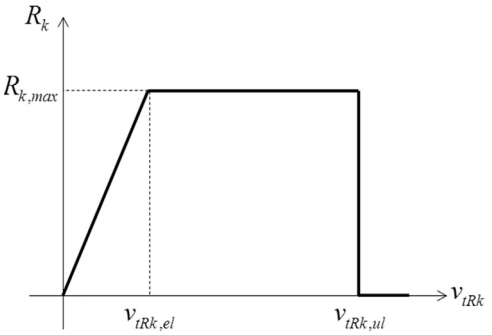

Fig. 2. Force-displacement curve governing the response of the generic k-th constrain acting on the tower.

supports acting along the axis of the tower. This approach may represent a simplification in some cases (e.g. a tower connected to a wall along only one of the edge of the tower) and fully 3D models would be needed to properly deal with these more peculiar situations.

The use of inverse analysis identification techniques, based on measurements of the dynamic behavior of the structure, has been shown to be a promising way to investigate the effectiveness of a constrain, which strictly depends on the degree of connection between the different structural elements, see [29–31].

In the proposed approach, the generic k-th restraint is modeled by an elasto-plastic curve with limited ductility, which expresses the force R_k transmitted by the support to the tower, as a function of the displacement v_{tRk} occurring in correspondence of the restrained section, see Fig. 2 and Eq. (2).

$$R_k = \begin{cases} \left(R_{k,\,\max}/v_{tRk,el}\right)\cdot v_{tRk} & \text{if } v_{tRk} \leq v_{tRk,el} \\ R_{k,\,\max} & \text{if } v_{tRk,el} < v_{tRk} < v_{tRk,ul} \\ 0 & \text{if } v_{tRk,ul} \leq v_{tRk} \end{cases} \quad (2)$$

The above relationship depends on three parameters: the maximum force $R_{k,\,\max}$ and the elastic and ultimate displacements, $v_{tRk,el}$ and $v_{tRk,ul}$ respectively.

2.2. Curvature versus bending moment curve

According to the above hypotheses and to the assumptions in Fig. 3, the strain distribution along the section can be expressed as:

$$\varepsilon_m(y) = \eta_t - y\chi_t \quad (3)$$

where the axial deformation η_t is defined with respect to the center of gravity G of the section.

Given the axial force N_{Ed} acting on the section (due to the self-weight of the tower) and a curvature $\chi_t = \bar{\chi}_t$, the axial equilibrium is imposed as:

$$N_t(\eta_t) = \int_A \sigma_m\left(\varepsilon_m(\bar{\chi}_t, \eta_t)\right)dA = N_{Ed} \quad (4)$$

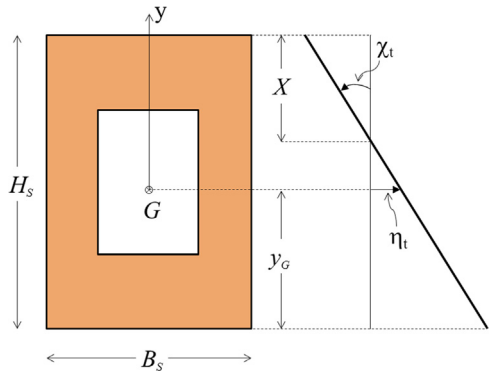

Fig. 3. Section of the tower and characteristics of deformation.

By exploiting a discretization of the section in triangular elements having three nodes each, the above equation is discretized as follows:

$$N_t(\eta_t) = \int_A \sigma_m\big(\varepsilon_m(\bar{\chi}_t, \eta_t)\big)dA \cong \sum_e \sum_j \sigma_{mej}\big(\varepsilon_{mej}(\bar{\chi}_t, \eta_t)\big)\frac{A_e}{3} = N_{Ed} \tag{5}$$

where: ε_{mej} is the strain computed by means of Eq. (3) at each Gauss point $j(j = 1 \dots 3)$ of each triangular element e, σ_{mej} is the corresponding stress computed trough Eq. (1) and A_e is the area of each triangular element.

The above equation is nonlinear in the unknown η_t and can be solved according to the following iterative Newton–Raphson scheme:

$$\eta_t^{i+1} = \eta_t^i - \left[\sum_e \sum_j \frac{A_e}{3} d_{mtej}\right]^{-1} \left[N_t^i - N_{Ed}\right] \tag{6}$$

d_{mtej} being the current tangent modulus of the masonry constitutive law, and N_t^i the axial stress resultant at the i-*th* iteration.

Once the value of η_t has been computed, the strain distribution is known and through Eq. (1) the moment $\bar{M}_t$ corresponding to the given axial force N_{Ed} and curvature $\bar{\chi}_t$ can be derived as:

$$\bar{M}_t = -\int_A y\sigma_m(\varepsilon_m)dA \cong -\sum_e \sum_j y_{ej}\sigma_{mej}(\varepsilon_{mej})\frac{A_e}{3} \tag{7}$$

By repeating the above steps for each curvature of a given set, the moment-curvature curve can be built numerically for each section.

2.3. Structural response evaluation

In view of the nonlinear geometric effects and the softening nature of the masonry constitutive law, the capacity curve of the structure may be characterized by a descending branch. In order to model this part of the response, we adopted a displacement controlled procedure, in which we applied a displacement δ_c at a certain section of the tower (named controlling point) and we formulated the problem in terms of the following unknowns: (i) the curvatures $\boldsymbol{\chi}_t = \left[\chi_{t1} \cdots \chi_{tM}\right]$ of M sections used to discretize the tower along its height, see Fig. 4; and (ii) the load factor α, which amplifies a predefined load distribution.

Given a vector of curvatures $\boldsymbol{\chi}_t = \left[\chi_{t1} \cdots \chi_{tM}\right]$, the corresponding vector of bending moment $\mathbf{M}_t^{\chi}(\boldsymbol{\chi}_t) = \left[M_{t1}^{\chi} \dots M_{tM}^{\chi}\right]$ is derived through the moment-curvature relationships above derived and the displacement $\mathbf{v}_t = \left[v_{t1} \dots v_{tM}\right]$ of each section (restrained or not) is computed by the principle of virtual work.

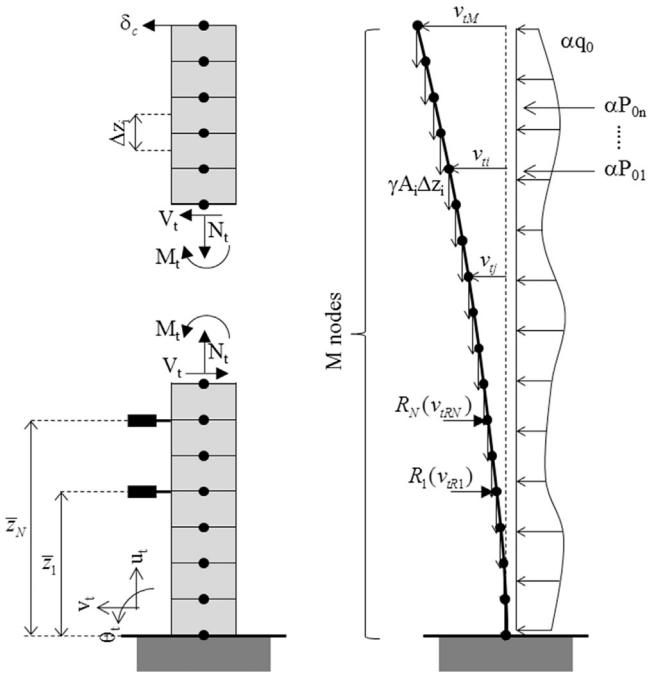

Fig. 4. Representation of the discretized tower and of the quantities considered in the numerical formulation proposed.

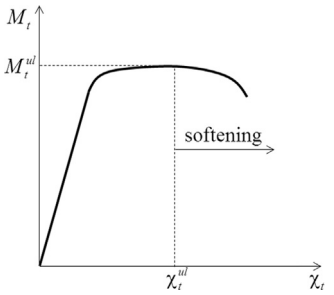

Fig. 5. Illustrative representation of a moment-curvature curve.

$$v_{ti} = \sum_{j=1}^{M} \hat{M}_{tij}\chi_{tj}\Delta z_j \quad \text{where:} \quad \begin{cases} \Delta z_j = \dfrac{H_T}{M-1} \;\forall\, j = 2 \dots M-1 \\ \Delta z_1 = \Delta z_M = \dfrac{1}{2}\dfrac{H_T}{M-1} \end{cases} \tag{8}$$

where: $\hat{\mathbf{M}}_{ti} = \left[\hat{M}_{ti1} \dots \hat{M}_{tiM}\right]$ is the bending moment distribution due to a unit force applied at the specific section i and H_T is the height of the tower.

In order to avoid curvature localization, induced by the softening constitutive law, provisions already adopted for RC structures are here considered (see, e.g. [32]). In particular, when a section (say $j = j_{crit}$) reaches its ultimate bending moment M_t^{ul} and enters the softening branch of the moment-curvature curve, see Fig. 5, the calculation of the sections displacement is performed according to Eq. (9), where the contribution of the curvature developed beyond χ_t^{ul} (onset of the softening branch), is spread over the assumed plastic hinge length l_p.

$$v_{ti} = \sum_{\substack{j=1 \\ (j \neq j_{crit})}}^{M} \hat{M}_{tij}\chi_{tj}\Delta z_j + \hat{M}_{tij_{crit}}\left[\chi_{tj_{crit}}^{ul}\Delta z_{j_{crit}} + \left(\chi_{tj_{crit}} - \chi_{tj_{crit}}^{ul}\right)l_p\right] \tag{9}$$

Eq. (9) represents a practical approach to circumvent the problem of curvature localization, and it has the great advantage of being easily implementable in the framework of the proposed approach.

As a function of the N displacements at the restrained sections, the corresponding reactions forces $\mathbf{R} = [R_1 \dots R_N]$ are derived through Eq. (2) and as a function of $\mathbf{R}$ and of the load amplification factor α, the corresponding vectors of bending moment $\mathbf{M}_t^{\mathbf{R}}(\mathbf{R}) = [M_{t1}^{\mathbf{R}} \dots M_{tM}^{\mathbf{R}}]$ and $\mathbf{M}_t^{\alpha}(\alpha) = [M_{t1}^{\alpha} \dots M_{tM}^{\alpha}]$, respectively, are derived by equilibrium equations. Finally, to take into account nonlinear geometric effects, the contribution to the bending moment distribution of the tower self-weight is expressed as a function of the displacement $\mathbf{v}_t$; i.e. $\mathbf{M}_t^{\mathbf{v}}(\mathbf{v}_t) = [M_{t1}^{\mathbf{v}} \dots M_{tM}^{\mathbf{v}}]$, where:

$$M_{ti}^{\mathbf{v}} = \sum_{j=i+1}^{M} \gamma \Delta z_j A_j (v_{tj} - v_{ti}) \tag{10}$$

The final system of $(M+1)$ nonlinear equations can be written as:

$$\underbrace{\begin{bmatrix} \mathbf{M}_t^{\chi}(\boldsymbol{\chi}_t) - \mathbf{M}_t^{\mathbf{R}}(\boldsymbol{\chi}_t) - \mathbf{M}_t^{\alpha}(\alpha) - \mathbf{M}_t^{\mathbf{v}}(\boldsymbol{\chi}_t) \\ v_{tc}(\boldsymbol{\chi}_t) \end{bmatrix}}_{\mathbf{Z}(\mathbf{Y})} = \underbrace{\begin{bmatrix} \mathbf{0} \\ \delta_c \end{bmatrix}}_{\mathbf{F}}$$

$$\text{where: } \mathbf{Y} = [\boldsymbol{\chi}_t, \alpha] \tag{11}$$

v_{tc} being the computed displacement of the controlling point.

The above nonlinear system is imposed in the framework of a step by step procedure, by discretizing the assigned displacement history into Q instants, run by index $q = 1 \dots Q$; and at each instant q, the equations are solved by means of the following iterative Newton-Raphson scheme, run by index k:

$$\mathbf{Y}_{k+1}^q = \mathbf{Y}_k^q - \left[\frac{\partial \mathbf{Z}}{\partial \mathbf{Y}}\Big|_k^q\right]^{-1} \left[\mathbf{Z}(\mathbf{Y}_k^q) - \mathbf{F}^q\right] \tag{12}$$

where the consistent tangent operator $\frac{\partial \mathbf{Z}}{\partial \mathbf{Y}}$ is derived in the following, by applying the derivative chain rule:

$$\left[\frac{\partial \mathbf{Z}}{\partial \mathbf{Y}}\right] = \begin{bmatrix} \frac{\partial \mathbf{M}_t^{\chi}}{\partial \boldsymbol{\chi}_t}\frac{\partial \boldsymbol{\chi}_t}{\partial \mathbf{Y}} - \frac{\partial \mathbf{M}_t^{\mathbf{R}}}{\partial \mathbf{R}}\frac{\partial \mathbf{R}}{\partial \mathbf{v}_t}\frac{\partial \mathbf{v}_t}{\partial \boldsymbol{\chi}_t}\frac{\partial \boldsymbol{\chi}_t}{\partial \mathbf{Y}} - \frac{\partial \mathbf{M}_t^{\alpha}}{\partial \alpha}\frac{\partial \alpha}{\partial \mathbf{Y}} - \frac{\partial \mathbf{M}_t^{\mathbf{v}}}{\partial \mathbf{v}_t}\frac{\partial \mathbf{v}_t}{\partial \boldsymbol{\chi}_t}\frac{\partial \boldsymbol{\chi}_t}{\partial \mathbf{Y}} \\ \frac{\partial v_{tc}}{\partial \boldsymbol{\chi}_t}\frac{\partial \boldsymbol{\chi}_t}{\partial \mathbf{Y}} \end{bmatrix} \tag{13}$$

Derivatives in matrix $\frac{\partial \mathbf{M}_t^{\chi}}{\partial \boldsymbol{\chi}_t}$ are computed by differentiating numerically the moment- curvature curves. Matrices $\frac{\partial \boldsymbol{\chi}_t}{\partial \mathbf{Y}}$ and $\frac{\partial \alpha}{\partial \mathbf{Y}}$ are Boolean matrices made of 0 and 1.

In order to improve convergence, especially when a sudden load drop occurs, recourse can be made to a line search algorithm to optimize the step size in the Newton-Raphson scheme:

$$\mathbf{Y}_{k+1}^q = \mathbf{Y}_k^q - \widehat{\zeta} \cdot \left[\frac{\partial \mathbf{Z}}{\partial \mathbf{Y}}\Big|_k^q\right]^{-1} \left[\mathbf{Z}(\mathbf{Y}_k^q) - \mathbf{F}^q\right]$$
$$\text{where: } \widehat{\zeta} = \arg\min_{\zeta}\left(\omega(\zeta) = \|\mathbf{Z}(\mathbf{Y}_{k+1}^q) - \mathbf{F}^q\|\right) \tag{14}$$

2.4. Load distribution

According to [14], the seismic force F_i acting on a single discrete mass W_i at a distance z_i from the base of a structure having total weight equal to W, can be computed as:

$$F_i = \alpha W \frac{z_i W_i}{\sum_j z_j W_j} \tag{15}$$

For a masonry structure with continuously and homogeneous distributed mass, the above formula can be written in terms of infinitesimal quantities as:

$$dF = \alpha \cdot W \frac{z dW}{\int_V z dW} = \alpha \cdot W \frac{z dV}{\int_V z dV} \tag{16}$$

where the load factor α is proportional to the acceleration induced by the earthquake and V is the volume of the tower. It follows that the seismic body force (i.e. the force per unit volume $\lambda(z)$) acting on the structure reads:

$$\lambda(z) = \frac{dF}{dV} = \alpha \cdot W \frac{z}{\int_V z dV} = \alpha \cdot \gamma \frac{z}{z_G} \tag{17}$$

z_G being the distance of the center of gravity of the tower from the base and γ the masonry specific self-weight.

The force per unit length $q(z)$ acting on the tower modeled as a beam reads:

$$q(z) = \lambda(z) \cdot A(z) = \alpha \cdot \gamma \frac{z}{z_G} A(z) \tag{18}$$

$A(z)$ being the area of each section.

Following the indications contained in many international codes, a uniform load distribution or a load distribution proportional to the first (or higher) mode shape may be defined similarly.

2.5. Algorithm for section discretization

In order to analyze masonry towers, having hollow arbitrary sections, a topological algorithm is here introduced to derive the discretization, based on triangular elements, of the sections starting from a three-dimensional finite element model of the whole tower based on tetrahedrons, being the latter usually available to perform the pushover analysis with commercial finite element codes.

Each 2D discretization is built up by intersection of the 3D elements with the plane of the section (of equation $z = \bar{z}$). The intersection of a tetrahedron with a plane gives rise or to a triangle with three nodes or to a quadrilateral figure with fours nodes, which can be split in two triangles, as visualized in Fig. 6. From the union of all these triangles the 2D discretization is derived.

Specifically, the proposed topological algorithm consists in the following steps:

- All the tetrahedrons intersected by the section of equation $z = \bar{z}$ are selected;
- For each of them the equation of the plane of each of the four faces is derived as follows:

$$a_i x + b_i y + c_i z + d_i = 0 \ (i = 1 \dots 4) \tag{19}$$

- The intersection of these four planes with the equation $z = \bar{z}$ gives rise to four straight lines having the following equations:

$$a_i x + b_i y + c_i \bar{z} + d_i = 0 \ (i = 1 \dots 4) \tag{20}$$

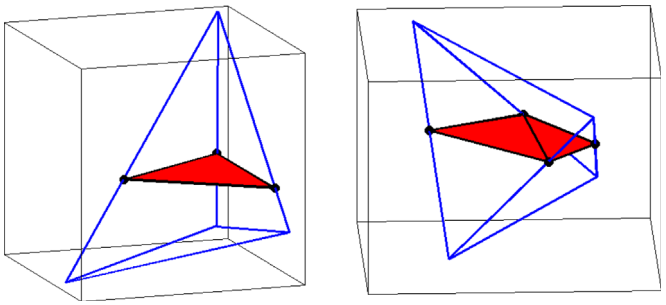

Fig. 6. Intersection of a tetrahedron with a plane, giving rise to a triangle or to a quadrilateral figure, which then can be split in two triangles.

- The intersection of these four straight lines among each other generates six nodes (belonging to the plane $z = \bar{z}$) whose coordinates (x, y) are derived by solving the following systems:

$$\begin{cases} a_k x + b_k y + c_k \bar{z} + d_k = 0 \\ a_j x + b_j y + c_j \bar{z} + d_j = 0 \end{cases}$$

with 6 combinations: $\dfrac{k}{j}\Big|\dfrac{111223}{234344}$ (21)

- Of these six nodes only those belonging to the tetrahedron are considered (three or four, see Fig. 6). If the nodes are three, a triangular element is directly obtained; vice versa from the four nodes, two triangular elements are derived and added to the bi-dimensional discretization.

3. Validation of the numerical procedure

In order to validate the proposed procedure, a real case was considered and benchmarking pushover analyses were performed with the commercial code Abaqus [27], whose results were then compared with the outcomes of the present approach.

This real case referred to the Gabbia Tower in Mantua, see [33], overlooking the historic center of the town. Construction techniques, materials, shape and location suggest that this construction dates back no later than the thirteenth century. The Gabbia Tower, about 54 m high, was built in solid masonry brick and has nearly square section with the sides 7.5 m long at the base. The load-bearing walls are about 2.4 m thick until the upper level (about 45.3 m from the base), then masonry walls thickness decreases to about 0.7 m.

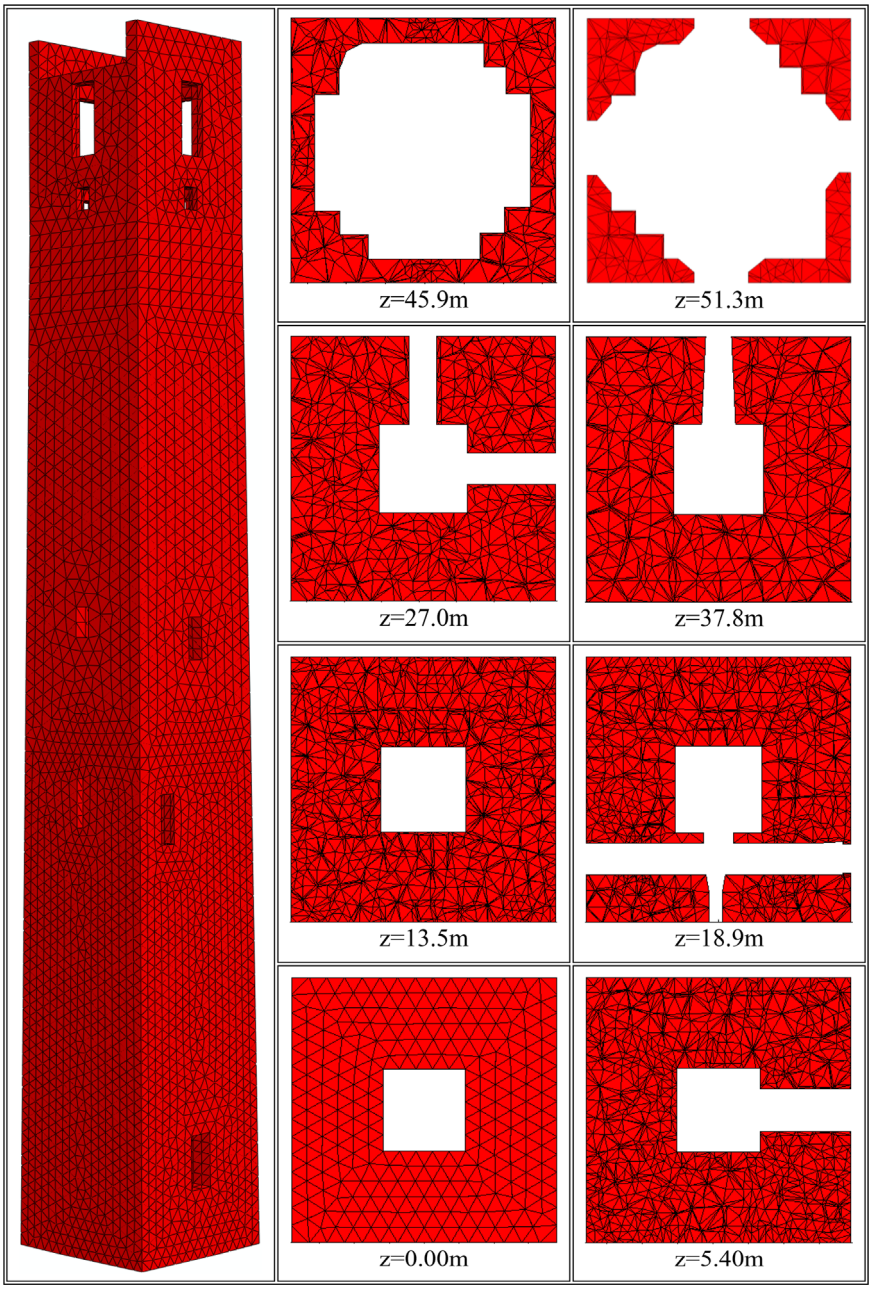

Fig. 7. Three dimensional finite element discretization, based on tetrahedron elements, adopted in the pushover analysis performed with Abaqus; and some of the derived triangular based discretizations of the sections for the pushover analysis performed with the proposed approach.

Fig. 7 visualizes the three dimensional finite element discretization of the tower, adopted to perform the benchmarking pushover analysis with the commercial code Abaqus, and the bi-dimensional discretization of some sections, obtained with the algorithm described in Section 2.5.

The compressive strength of the material was defined on the basis of what suggested by the Italian Code [13] in Annex C8A.2 for a knowledge level of 1. Based on table C8A.2.1 a compressive strength and modulus of elasticity equal to 2.4 MPa and 1500 MPa, respectively, were assumed for solid brick and lime mortar. Applying then a confidence factor CF equal to 1.35 and the additional correction factor, according to the table C8A.2.2 in [13], of 1.5 for a mortar of good quality, we obtained a final design compressive strength equal to $f_{mc}=2.67$ *MPa*. The tensile strength of the masonry was assumed equal to $f_{mt}=0.09$ MPa.

The three dimensional CAD geometrical model (.sat format) of the tower was imported into the finite element program Abaqus [27]. As a compromise between the conflicting requirements of reasonable computing time and accuracy of the solution, a finite element discretization of 99,108 four nodes elements, for a total number of 20,443 $\times$ 3 = 61,329 degrees of freedom, was adopted. Perfect connection was assumed between perpendicular walls.

In Abaqus, the concrete damage plasticity model (CDP) was adopted for masonry. This is characterized by: (1) linear and isotropic behavior in the elastic regime and (2) plastic damageable behavior in the nonlinear range, taking into account the difference of compressive and tensile strengths and the softening once the strength of the material is reached. The plasticity-based damage model adopted assumes that the main failure mechanisms are tensile cracking and compressive crushing. For more details about the adopted constitutive law, see [6,8,27].

Abaqus analysis was performed in two steps: the self-weight was initially applied and then the body force $\lambda(z)$, defined in Eq. (17), was applied along the height of the tower.

Table 1, in relation to Fig. 1, reports the uniaxial stress-strain relationship properties adopted for the analyses with Abaqus and the present formulation.

Fig. 8 visualizes the moment-curvature curves of the sections represented in Fig. 7, obtained according to the procedure described in Section 2.2. Obviously, the more the section is close to the base of the tower, the larger the axial force induced by the self-weight, the higher the ultimate bending moment and the smaller the ultimate curvature.

The load distribution, applied in the proposed procedure, is visualized in Fig. 9. This was computed according to Eq. (18), assuming the parameters reported in Table 2. The piecewise linear aspect is due to a non-uniform cross section and to the influence of the openings along the height of the tower.

A first parametric study was performed, in which l_p was kept equal to 4.0 m and different along the height discretizations (M = 50 100 – 150 200 were adopted to show the efficiency of the provision adopted to avoid curvature localization, see Fig. 10. The effect of large displacement is also shown in this parametric study, which caused a 6% decrease of the maximum shear base force and a very small variation in the maximum displacement.

While different expressions, characterized by large variations, are proposed in literature to estimate plastic hinge length for reinforced concrete elements (see e.g. [32,34–37]), similar formulations do not exist, to the best of the authors' knowledge, for unreinforced masonry structures. A preliminary guidance about its value can be derived by adopting the same approaches proposed for reinforced concrete, but without considering the contribution of the reinforcement. According to [32] and references therein, l_p can be estimated either as $l_p = 0.5H_S = 3.75$ m or $l_p = 0.08H_T = 4.32$ m. Applying the proposal in [36], it follows that $l_p = 0.25H_S = 1.875$ m; while following [37], $0.15H_S(=1.125m) < l_p < 0.25H_S$ (=1.875 m). However, differently from classical approaches for RC structures, the assumed plastic hinge length l_p is here multiplied by the curvature developed beyond χ_t^{ul} (i.e. the onset of the softening branch, which has a more objective definition than the elastic limit used for RC structures, see [35]). Therefore larger values of l_p have to be expected.

In order to investigate the influence of the plastic hinge length on the response of the structure and to define a reliable value for

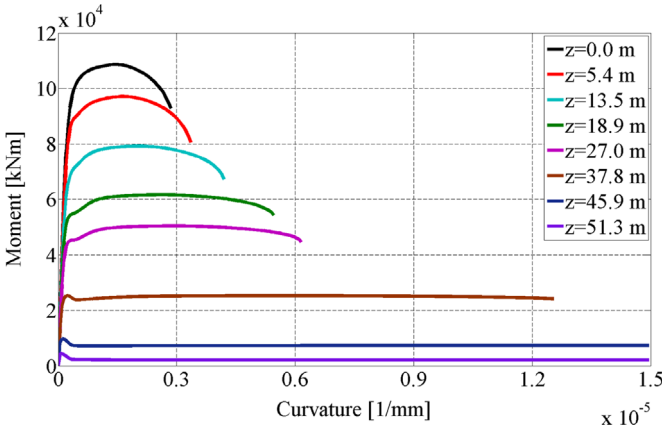

Fig. 8. Moment-curvature curves of the sections represented in Fig. 7.

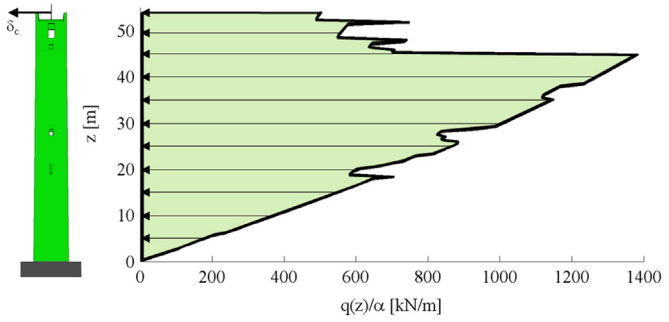

Fig. 9. Distributed load $q(z)$ computed according to Eq. (18).

Table 2
Parameters of the Gabbia tower adopted to compute the load distributions $\lambda(z)$ and $q(z)$.

V (m^3)	γ (kN/m^3)	W (kN)	z_G (m)
2172	18	39,096	23.4

Table 1
Uniaxial stress-strain relationship properties adopted for both the analyses with Abaqus and the present formulation.

E_m	f_{mc}	f_{mt}	$\varepsilon_{mc1}=f_{mc}/E_m$	ε_{mc2}	ε_{mcu}	$\varepsilon_{mt1}=f_{mt}/E_m$	ε_{mtu}
1500 MPa	2.67 MPa	0.09 MPa	0.001778	0.0035	0.0100	0.000025	0.00150

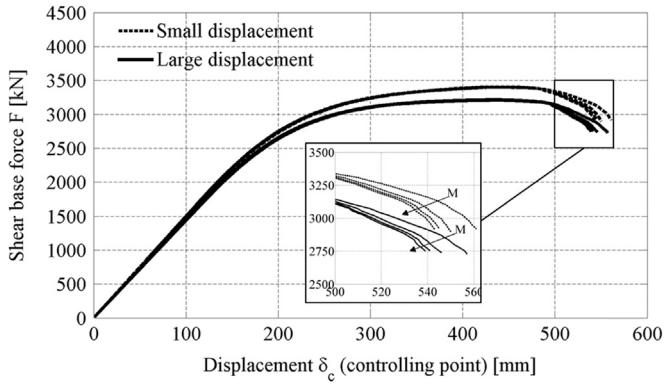

Fig. 10. Pushover curves computed, without and with large displacement effects, assuming $l_p = 4.0$ m and different tower discretizations ($M = 50 - 100 - 150 - 200$).

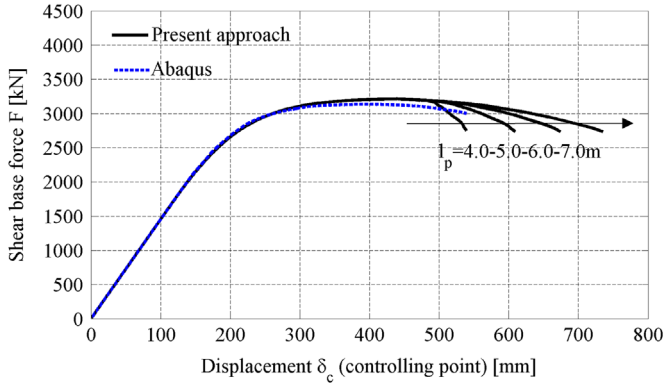

Fig. 11. Pushover curves computed, with geometric nonlinear effects, with Abaqus and with the present approach assuming different plastic hinge lengths.

this parameter, a second parametric study was performed with respect to l_p, whose results are visualized in Fig. 11, in terms of load-displacement curves, computed with the proposed procedure and with Abaqus. For each l_p assumed, the results are in good agreement in terms of maximum force and failure mechanism, the latter consisting in a flexural hinge at the base of the tower, see Fig. 12. Plastic hinge length exerts its influence on the softening portion of the curve only, i.e. on the maximum displacement. By comparison with the 3D finite element analysis, it seems that $l_p = 4.0$ m can be taken here as the most reliable value of this parameter in this initial presentation of the methodology.

This example also pointed out the great reduction of computing time achieved with the proposed approach with respect to the commercial code. Specifically, the computing time for one push-over analysis required by Abaqus and the proposed approach are about 5 h and 20 min, respectively, of CPU time by a computer i7-2600 with 3.40 GHz processor and 16 GB of RAM.

In order to model the effect of the buildings surrounding the tower, without the aim of performing an exhaustive vulnerability analysis, the structure is now modeled imposing a restraint acting on the tower at a distance of $\bar{z}_1 = 18.9m$ from the base, see Fig. 4, representing the effect of the floors and vaults supported by the tower.

On the basis of the geometry and material properties of the surrounding buildings, elastic and ultimate displacements of the constrain were estimated equal to $v_{tR1,el} = 0.05$ m and $v_{tR1,ul} = 0.10$ m, respectively, and the maximum force equal to $R_{1,\,max} = 1600$ kN. The cases of no and perfect constrain are also considered for comparison purposes.

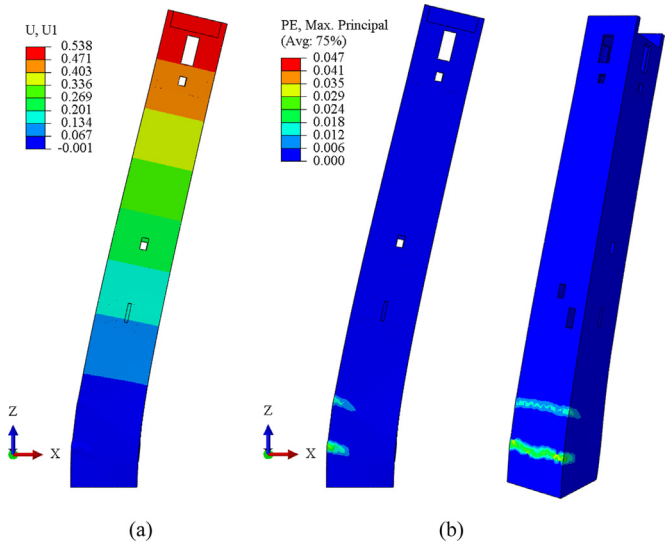

Fig. 12. Results of the pushover analysis, at the ultimate displacement, performed with Abaqus in terms of: (a) displacement along the loaded direction (scale factor x20); (b) maximum inelastic principal strain distribution.

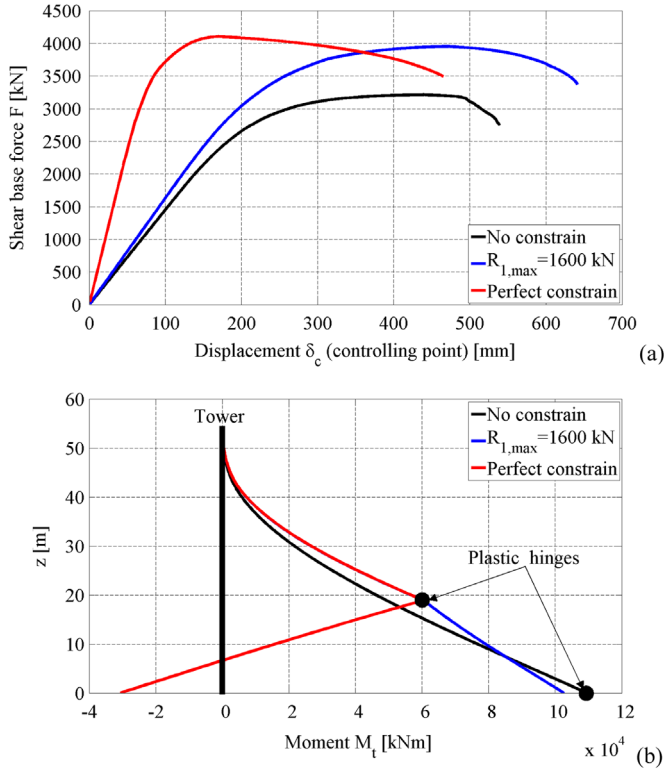

Fig. 13. (a) Pushover curves obtained considering different degrees of constrain of a support acting on the tower; (b) bending moment distributions computed in correspondence of the final load achieved in the pushover curves represented in (a).

As expected, the presence of a support induced in the pushover curve an increase of both the initial stiffness and the maximum force achieved, see Fig. 13(a); and caused the plastic hinge to occur at the constrain position instead of the base, see Fig. 13(b). While in case of damaging constrain the bending moment distribution is only slightly different from the case of no constrain; a perfect constrain induced also a sign reversal in the bending moment distribution.

3.1. Probabilistic analysis

It is well known that material properties of existing masonry are characterized by a large variability. For this reason, the proposed procedure is here adopted to perform a probabilistic investigation of the influence of the material properties uncertainties on the tower structural response. The parameters involved in this Monte Carlo study are reported in Table 3 with the assumed probabilistic characterization (see, e.g. [19,38,39]), while the other parameters are kept constant and equal to the values reported in Table 1. Three thousand combinations were then randomly extracted assuming a frequency normal distribution for each parameter. Monte Carlo simulation was split over 7 processors of a computer i7-2600 with 3.40 GHz processor and 16 GB of RAM and the total computing time was equal to about 6 days.

Table 3
Probabilistic characterization of the parameters involved in the Monte Carlo simulation, and of the results achieved.

	Input data				Output data	
	E_m [MPa]	f_{mc} [MPa]	$\mu_1 = \mu_2$	l_p [m]	F_{max} [kN]	d_{max} [mm]
Mean value	1500	2.67	2.50	4.0	3155	579
Stand. Deviat	300	0.53	0.50	0.8	270 (9%)	231 (40%)
Correlation	0.80		0.50		0.54	

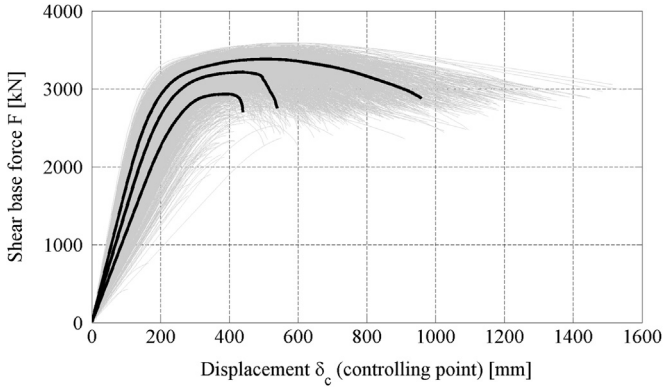

Fig. 14. Results of the stochastic pushover analysis, with identification of the curves based on mean and mean ± standard deviation parameter values.

Fig. 14, which visualizes all the pushover curves obtained by the $3 \cdot 10^3$ combinations, shows a large variability of the tower structural response, particularly in terms of ultimate displacement.

Fig. 15 visualizes the probability density and cumulative distribution functions of both the maximum force F_{max} and displacement d_{max}, which were taken as most representative parameters of the structural response and whose mean value and standard deviation are reported in Table 3. Bars represent the numerical results of the Monte Carlo simulation while continuous lines represent the theoretical values based on a Weibull and Lognormal distributions assumed for F_{max} and d_{max}, respectively. In particular, from these results it is possible to observe a rather large variability of the maximum displacement (characterized by a standard deviation equal to 40% of the mean value), which represents a crucial parameter in the seismic vulnerability assessment of the structure. This result underlines, as in previous studies (see, e.g [38,39] and references therein), the necessity to take into account the statistical variability of masonry parameters, for seismic vulnerability assessment purposes.

Fig. 16 visualizes the convergence curves, with respect to the number of Monte Carlo extractions, of mean and standard deviation values of F_{max} and d_{max}, respectively. From this figure it is possible to observe that in this case 10^3 combinations were enough in order to guarantee convergence of the probabilistic analysis.

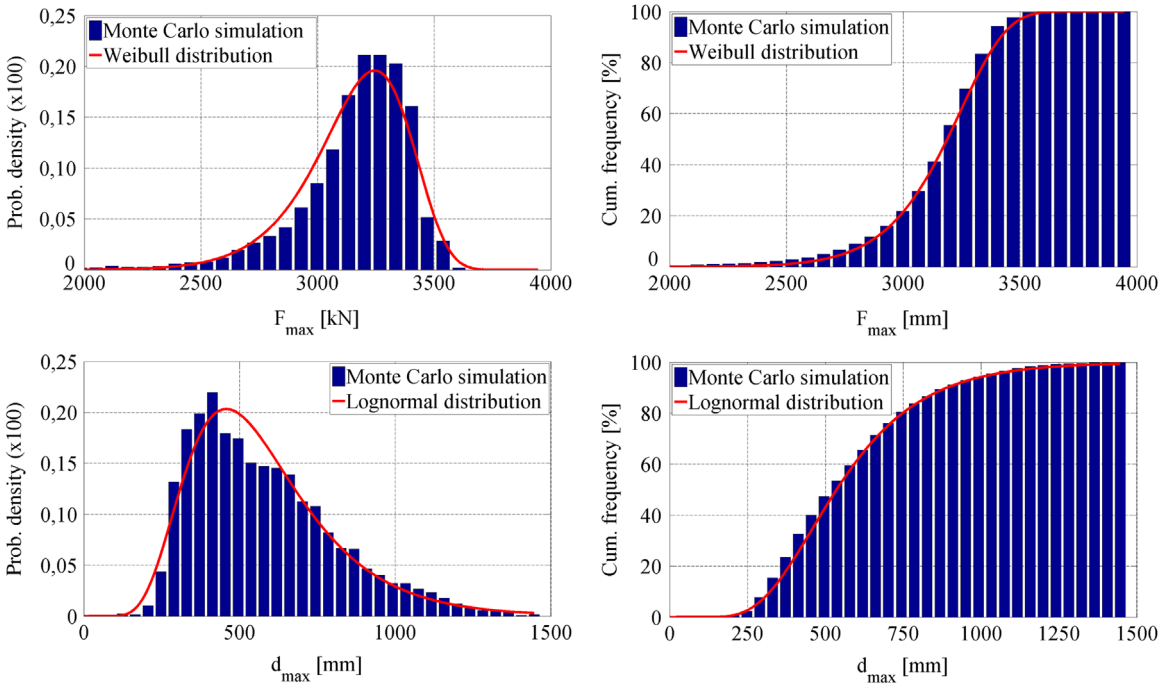

Fig. 15. Probability density and cumulative distributions computed by Monte Carlo simulation and their analytical representations by Weibull and Lognormal curves for F_{max} and d_{max}, respectively.

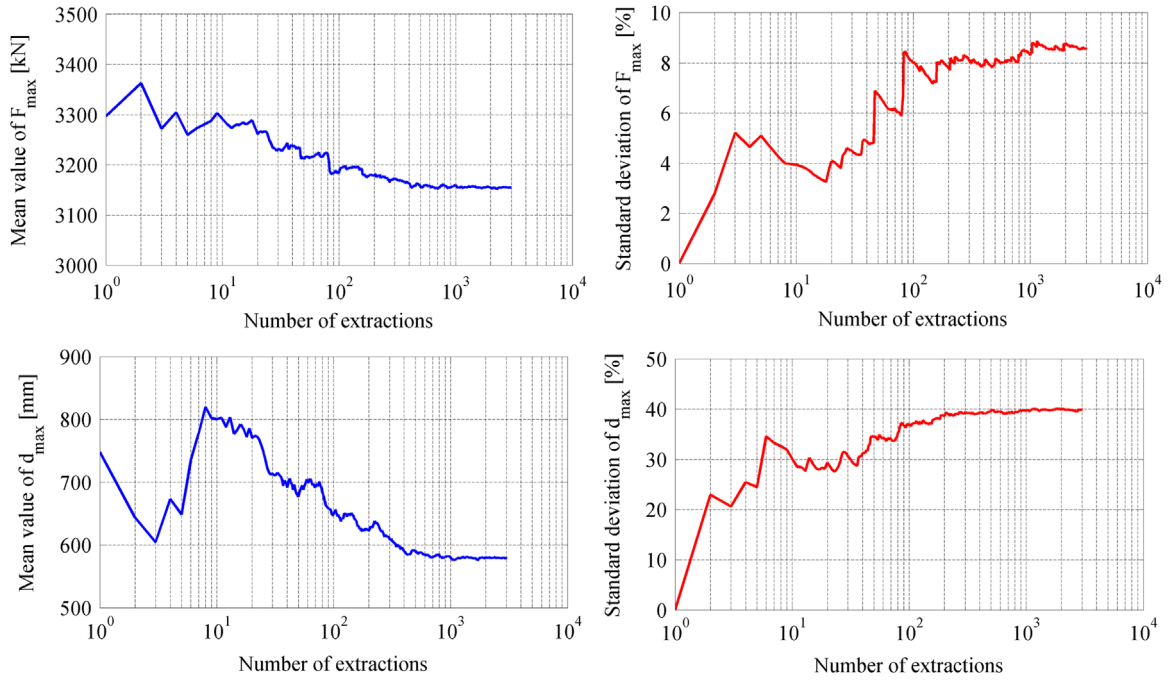

Fig. 16. Convergence of mean and standard deviation values of F_{max} and d_{max}, respectively.

4. Closing remarks

In this paper a numerical procedure is proposed in order to perform force driven pushover analyses of masonry towers with displacement control.

The proposed procedure presents the following advantages: i) it takes into account geometrical and material nonlinear effects and it is robust with respect to sudden or gradual load drops, which permit to follow easily the post peak softening branch of the structural response; ii) the concept of plastic hinge, necessary to avoid curvature localization arising in view of the adopted softening constitutive law, can be easily implemented; iii) the real geometry of the tower, characterized by hollow arbitrary sections (including openings and changes of section) can be considered.

Benchmarking pushover analyses were performed with the commercial code Abaqus in relation to a real case (the Gabbia Tower in Mantua) which proved the accuracy and reliability of the results obtained with the present formulation and the noteworthy reduction of computing time.

It was pointed out the great influence of the assumed plastic hinge length on the ultimate displacement achieved, which in turn plays a crucial role when the capacity curve has to be compared with the seismic demand, for seismic vulnerability assessment purposes. Since to the best of the authors' knowledge, formulations for plastic hinge length do not exist for unreinforced masonry structures, an estimation of this parameter was done by comparison with 3D finite element analyses, but its effect on the final response of the structure requires further explanation and validation.

The influence of the uncertainty of the plastic hinge length and other material parameters, on the tower structural response, was investigated by performing a probabilistic analysis, which was made possible by the considerable saving of computing time achieved by the proposed approach, with respect to standard 3D finite element analyses. Indeed, the efficiency of the proposed numerical procedure turned out to be particularly relevant in this probabilistic study, which required results from a large number of simulations, to reach conclusions valid from a statistical point of view.

This numerical model is not intended to provide an exhaustive seismic vulnerability analysis of a masonry tower. Local failure mechanisms induced by peculiar crack patterns or the presence of vaults and large openings, which often characterize the collapse mechanisms in masonry towers, see [40], have still to be checked by proper methods. However, this numerical model is able, as long as the assumption of plane section is valid, to consider the main features influencing the global structural behavior of a masonry tower, as material nonlinear and softening behavior, large displacements, hollow generic section. This numerical approach has to be considered complementary to more sophisticated and time consuming 3D finite element analyses, able to deal in principle with the whole complexity of a structure. This approach may be adopted when the computing time represents a crucial item, such as in a probabilistic analysis or when, following a procedure suggested in [14], a quick initial vulnerability assessment of the collapse mechanisms induced by the first modes of vibration is required, in order to figure out the possible need for deeper investigations.

References

[1] Valluzzi MR, Cardani G, Saisi A, Binda L, Modena C. Study of the seismic vulnerability of complex masonry buildings. Adv Archit Ser 2005;20:301–10.
[2] Ramos LF, Lourenço PB. Modeling and vulnerability of historical city centers in seismic areas: a case study in Lisbon. Eng Struct 2004;26(9):1295–310.
[3] Lagomarsino S. Damage assessment of churches after L'Aquila earthquake. Bull Earthq Eng 2009;10(1):73–92.
[4] Foraboschi P. Church of San Giuliano di Puglia: seismic repair and upgrading. Eng Fail Anal 2013;33:281–314.
[5] Biolzi L. Evaluation of compressive strength of masonry walls by limit analysis. J Struct Eng 1988;114(10):2179–89.
[6] Barbieri G, Biolzi L, Bocciarelli M, Fregonese L, Frigeri A. Assessing the seismic vulnerability of a historical building. Eng Struct 2013;57:523–35.
[7] Peña F, Lourenço PB, Mendes N, Oliveira DV. Numerical models for the seismic assessment of an old masonry tower. Eng Struct 2010;32(5):1466–78.
[8] Acito M, Bocciarelli M, Chesi C, Milani G. Collapse of the clock tower in Finale Emilia after the May 2012 Emilia Romagna earthquake sequence: Numerical insight. Engineering Structures. Vol. 72; 2014, p. 70–91.
[9] Giordano A, Mele E, De Luca A. Modelling of historical masonry structures: comparison of different approaches through a case study. Eng Struct 2002;24 (8):1057–69.
[10] Pintucchi B, Zani N. Effectiveness of nonlinear static procedures for slender masonry towers. Bull Earthq Eng 2014;12(6):2531–56.
[11] Fajafar P, Gašperšič P. The N2 method for the seismic damage analysis of RC.

Build Earthq Eng Struct Dyn 1996;25(1):31–46.
[12] Fajafar P. Capacity spectrum method based on inelastic demand spectra. Earthq Eng Struct Dyn 1999;28(9):979–93.
[13] Nuove norme tecniche per le costruzioni e Circolare esplicativa. Ministero delle Infrastrutture (GU n.29 04/02/2008). Rome, Italy; 14/01/2008.
[14] Linee Guida per la valutazione e la riduzione del rischio sismico del patrimonio culturale. Italy: Ministero per i beni e le attività culturali MiBAC; 2011.
[15] Penelis GG. An efficient approach for pushover analysis of unreinforced masonry (URM) structures. J Earthq Eng 2006;10(3):359–79.
[16] D'Ayala D, Ansal A. Non linear push over assessment of heritage buildings in Istanbul to define seismic risk. Bull Earthq Eng 2012;10(1):285–306.
[17] Ceroni F, Pecce M, Sica S, Garofano A. Assessment of seismic vulnerability of a historical masonry building. Buildings 2012;2(3):332–58.
[18] Meireles H, Bento R, Cattari S, Lagomarsino S. Seismic assessment and retrofitting of Pombalino buildings by pushover analyses. Earthq Struct 2014;7(1):57–82.
[19] Foti D. A new experimental approach to the pushover analysis of masonry buildings. Comput Struct 2015;147:165–71.
[20] Ceroni F, Pecce M, Manfredi G. Seismic assessment of the bell tower of Santa Maria del Carmine: problems and solutions. J Earthq Eng 2010;14(1):30–56.
[21] Casolo S, Milani G, Uva G, Alessandri C. Comparative seismic analysis on ten masonry towers in the coastal Po Valley in Italy. Eng Struct 2013;49:465–90.
[22] Milani G, Casolo S, Naliato A, Tralli A. Seismic assessment of a medieval masonry tower in northen italy by limit, nonlinear static, and full dynamic analyses. Int J Archit Herit 2012;6(5):489–524.
[23] Casolo S, Uva G. Nonlinear analysis of out-of-plane masonry façades: Full dynamic versus pushover methods by rigid body and spring model. Earthq Eng Struct Dyn 2013;42(4):499–521.
[24] D'Ambrisi A, Mariani V, Mezzi M. Seismic assessment of a historical masonry tower with nonlinear static and dynamic analyses tuned on ambient vibration tests. Eng Struct 2012;36:210–9.
[25] Chopra AK, Goel RK. A modal pushover analysis procedure for estimating seismic demands for buildings. Earthq Eng Struct Dyn 2002;31(3):561–82.
[26] Ramm E. Strategies for tracing the non-linear response near limit points. In: Wunderlich W, Stein E, Bathe KJ (Eds.), Nonlinear finite element analysis in structural mechanics. Springer Berlin Heidelberg; 1981, p. 63–89.
[27] ABAQUS/Standard. Theory and users manuals, release 6.10-1. Pawtucket, RI, USA: HKS Inc.; 2007.
[28] Foti D. On the numerical and experimental strengthening assessment of tufa masonry with FRP. Mech Adv Mater Struct 2013;20(2):163–75.
[29] Friswell MI, Mottershead JE. Finite element model updating in structural dynamics. Dordrecht: Springer Science & Business Media; 1995.
[30] Diaferio MD, Foti D, Giannoccaro NI. Non-destructive characterization and identification of the modal parameters of an old masonry tower. IEEE Workshop on environmental, energy and structural monitoring systems. Naples, Italy, 17–18 September; 2014.
[31] Capecchi D, De Angelis M, Sepe V. Modal model identification with unknown nonstationary base motion. Meccanica 2004;39(1):31–45.
[32] Inel M, Ozmen HB. Effects of plastic hinge properties in nonlinear analysis of reinforced concrete buildings. Eng Struct 2006;28(11):1494–502.
[33] Saisi A, Gentile C. Post-earthquake diagnostic investigation of a historic masonry tower. J Cult Herit 2015;16(4):602–9.
[34] Corley WG. Rotational capacity of reinforced concrete beams. J Struct Div ASCE 1966;92(5):121–46.
[35] Park R, Priestley MJN, Gill WD. Ductility of square confined concrete columns. J Struct Div ASCE 1982;108(4):929–50.
[36] Bae S, Bayrak O. Plastic hinge length of reinforced concrete columns. ACI Struct J 2008;105(3):290–300.
[37] Shedid MT, El-Dakhakhni WW. Plastic hinge model and displacement-based seismic design parameter quantifications for reinforced concrete block structural walls. J Struct Eng 2014;140(4) 04013090-1-04013090-15.
[38] Salvatori L, Marra AM, Bartoli G, Spinelli P. Probabilistic seismic performance of masonry towers: general procedure and a simplified implementation. Eng Struct 2015;94:82–95.
[39] Rota M, Penna A, Magenes G. A methodology for deriving analytical fragility curves for masonry buildings based on stochastic nonlinear analyses. Eng Struct 2010;32(5):1312–23.
[40] Cattari S, Degli Abbati S, Ferretti D, Lagomarsino S, Ottonelli D, Tralli A. Damage assessment of fortresses after the 2012 Emilia earthquake (Italy). Bulletin of Earthquake Engineering. Vol. 12; 2014, p. 2333–65.